Vibration transmission in a double-leaf plate with random rigidities and junctions

Hyuck Chung

School of Computing and Mathematical Sciences, Auckland University of Technology, Auckland, New Zealand

ABSTRACT

Predicting vibrations of composite structures such as double-leaf plates is difficult because of the large number of components. In the low and high frequency ranges, the components may be homogenized, so that a structure becomes simple enough to be mathematically and computationally tractable. However the vibrations in the mid-frequency range cannot be predicted using such methods because the wavelengths are comparable to the size of the components and junctions between components. In this paper a double-leaf plate is modelled using the Kirchhoff plate and Euler beam theories. The elastic moduli and junctions are allowed to be inhomogeneous. These inhomogeneities are simulated as smooth random functions rather than discrete random numbers. The random functions are incorporated into the model using the variational formulation. Response of the plates are studied with various parameters.

INTRODUCTION

This paper shows how to compute vibrations of rectangular elastic plates with inhomogeneous rigidity. The elastic plates here include a single plate with various random stiffness distributions and a double-leaf plate (DLP) with irregular junctions between the plates and the reinforcement beams. Figures 1 and 2 show simple depictions of the structures studied in this paper. Numerical simulations will be used to study the variations of the fundamental frequencies of the single-plate when the plate has different kinds of random rigidity. The DLP will be studied using the same randomness in addition to the randomness in the junctions. The displacement of the two plates will be computed, and then the transmission loss between the two plates will be studied.

Some elastic plates with random material properties such as rigidity or density have been studied using the theory of random matrices. In order to use random matrix theory, a random parameter must give a stiffness matrix that has independent-identically distributed random variables as its elements. The random matrix theory can be rather technical and it usually deals with distributions of whole eigenvalues of very large matrices, whose elements are identical independent random values. In this paper the stiffness matrices are small because of the finite size and the simple rectangular shape of the plates. Furthermore the elements the matrix are correlated because the rigidity here can have auto-correlation over the plates and beams. Figure 1 shows an example of discrete random rigidity distributed over the grid on the plate. The rigidity D_{pg} is a random variable with some probability density function (PDF). It is simple to run numerical experiments to confirm that the eigenvalues or the fundamental frequencies are normally distributed when D_{pq} has either a uniformly or a normally distributed PDF. However the distribution of the fundamental frequencies behaves differently when the rigidity varies smoothly over the plate with smooth power spectral density.

The number of components in a DLP, which have to be connected in some ways, makes it difficult to construct mathematical model of DLPs. Although DLPs are mathematically difficult to deal with, they are attractive in real-life. DLPs have high strength-to-weight ratio, and are used in many lightweight

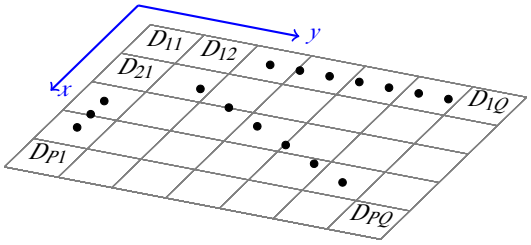

Figure 1. Depiction of the randomly distributed rigidity.

constructions. However DLPs usually have poorer sound insulation performance than single-layer heavy plates of equivalent thickness. A difficulty of modelling a DLP is that components interact in complex and unpredictable ways. There are various methods of joining the two component, such as nails and glue, which are difficult to represent mathematically. An often used modelling method is the finite element method (FEM), which requires detailed descriptions of the junction between a plate and a beam, e.g., nail's reaction to forces and effects on the surrounding components. In this paper the junctions are modelled by the amount of energy required for any particular way of deformation of the neighbouring components. In other words, the amount of energy at a junction will be large (or small) if the bonding is strong (or weak).

In the next section the displacement of the plates is found using the Fourier expansion of the solution, which is possible here because of the rectangular shape of the DLP. The Fourier expansion method requires less computation than FEM. Furthermore the conditions at the junctions, which must be functions of spatial variable(s), can also be included in the variational formulation as the Fourier expansion. This reduces the computation time. These reductions of computation time lead to faster Monte-Carlo simulations using the random functions for the parameters, which are elasticity modulus of the plates and junction rigidities. It may be computationally impossible to use the FEM to perform thousands of Monte-Carlo simulations over a wide frequency range without a super computer. Whereas all results shown here are produced using MatLab on an average desktop PC.

Deterministic models of plates-and-beams can predict the vibrations of DLPs of various types as shown in, for example (Brunskog, 2005; Chung and Emms, 2008; Mace, 1980a,b,c; Wang et al., 2005). These papers have also shown shortcomings of deterministic models at higher frequencies. There have been studies of more idealized models, such as periodically reinforced plate (beam) of infinite extent, or infinite plates (beams) with slightly randomized stiffeners. As an alternative to the FEM, the statistical energy analysis (SEA) has been developed and used often to study the wave propagation through complex structures. A well used textbook on the subject may be (Lyon, 1975). In the SEA, a structure is divided into subsystems that interact with their neighbouring systems. Two neighbouring subsystems are related by a loss factor, which is determined either from experiments or theoretical modelling. In (Craik, 2000a,b), various types of junctions of DLPs are considered, and experimental measurements and theoretical predictions are compared. SEA can predict the high frequency surface vibration. Some argument against using the SEA in the low-to-mid-frequency range is given in (Fahy, 1994). An example of SEA's unsuitability in predicting energy propagation in a DLP is given in (Brunskog and Chung, 2011). The SEA would be a suitable tool for the vibrations of the frequency range studied in this paper.

One can find variations in vibrations of composite structures that are apparently identical. The discrepancy may come from the manufacturing inconsistencies or random inhomogeneities in the components themselves. The unpredictability of the vibrations of composite structures have been known for many years (see (Hodges and Woodhouse, 1986)), and modelled using various methods, such as perturbation, scattering, asymptotic methods. All of these methods assume the irregularities in the structure to be small compared to the wavelengths. This is not true for most engineered products, whose components have the similar dimensions to the wavelengths at mid frequencies. The random rigidities of the plates and the junctions here are not limited to small values.

The random parameters that are studied in this paper are rigidity of the plates and the junctions. The random parameters are simulated as continuous smooth random functions (or process) over the length and/or the width of the DLP. The realizations of the random functions are computed using the predetermined power spectral density (PSD) and PDF. The method of simulating such random functions (or processes) are borrowed from the researches in the signal processing community (Kay, 2010). Although it is theoretically possible to generate random functions with any PDF and PSD, the functions in this paper are limited to Gaussian distribution for simplicity. The question of any dependence on (or lack of them) the PDF and the PSD of the inhomogeneities is still open.

MODELLING AND MATHEMATICAL FORMULATION

The method of solutions comes directly from Hamilton's principle for elastic plates (see (Shames and Dym, 1991)). The Lagrangian for the plate is derived from the kinetic and strain energies of the plate as it vibrates. Hamilton's principle states that when there is an external force that causes the plate to vibrate the total energy (Lagrangian) of the plate satisfies the following equation for the first variation of the time integral of the Lagrangian.

$$\delta^{(1)} \int_{t_1}^{t_2} \left(\mathscr{T} - \mathscr{V} - \mathscr{U} \right) dt = 0 \tag{1}$$

where $\mathscr{T}$, $\mathscr{V}$ are the kinetic and strain energies and $\mathscr{U}$ is the work done to the plate by the external force. For simplicity the simple harmonic oscillation of a thin plate is considered here. Thus the solution, the vertical displacement of the mid-plane of the plate, is given by the real function $\mathbf{Re}\left[w(x,y)e^{\mathrm{i}\,\omega t}\right]$, where $\omega = 2\pi\alpha$ is the radial frequency for the frequency α in Hz. Then mathematical formulations can be simplified for the function $w(x,y)$ because of the linearity of the thin-plate theory. The time integral in Equation (1) is now unnecessary. The displacement $w(x,y)$ will be defined for $(x,y) \in [0,A] \times [0,B]$, which is the size of the rectangular plate here. Hence the terms in the integral are completely determined by the vertical displacement of the plate. The derivation of the solution that satisfies Equation (1) will be shown in the following.

The strain energy and kinetic energy of a plate with non-moving boundaries are

$$\mathscr{V} = \frac{1}{2} \int_0^A \int_0^B D(x,y) \left| \nabla^2 w(x,y) \right|^2 dxdy \tag{2}$$

$$\mathscr{T} = \frac{\rho h \omega^2}{2} \int_0^A \int_0^B |w(x,y)|^2 dxdy \tag{3}$$

where $D(x,y) = E(x,y)h^3 / \left(12\left(1-\nu^2\right)\right)$ is the flexural rigidity, and h, E, and ν are the plate thickness, Young's modulus and Poisson's ratio, respectively. Note that the effects of rotation are neglected in $\mathscr{T}$. The work done to the plate is given by the following integral when the external force is distributed over the plate by the function $p(x,y)$.

$$\mathscr{U} = \int_0^A \int_0^B p(x,y) w(x,y)\, dxdy \tag{4}$$

Some readers may be more familiar with the following partial differential equation for the displacement resulting from the equation of motion derived from Equation (1).

$$\nabla^2 \left(D(x,y) \nabla^2 w(x,y) \right) - \omega^2 \rho h w(x,y) = p(x,y)$$

The above equation can be useful when an analytical solution can be considered. In this paper, the integral form is used because of the irregular structural properties requires a numerical solution method.

Double-leaf plates

An additional plate joined by parallel reinforcement beams can be included in the modelling using the same variational formulation. The additional components' strain and kinetic energies can be included in the integral form in Equation (3). The junctions between components may also be treated as an additional energy contribution due to the constraint in the movement of the components. Thus this model does not consider the plates and the beams to be simply sitting on top of each other. Figure 2 shows the modelling regime for the DLP.

The displacements of the top and the bottom plates are denoted by $w_1(x,y)$ and $w_3(x,y)$, respectively. The displacements of the beams are denoted by $w_2(x,j)$, where $j = 1,2,...,S$ indicates jth beam located at $y = y_j$. Note that the beams here are assumed to be always in contact with the plates. It is possible to add more degrees of freedom to the beams as shown in (Chung, 2012), though only the lateral slippage between the plates and the beams is considered here. The kinetic and the strain energies of the plates have the same formulas as Equation (3) for w_3.

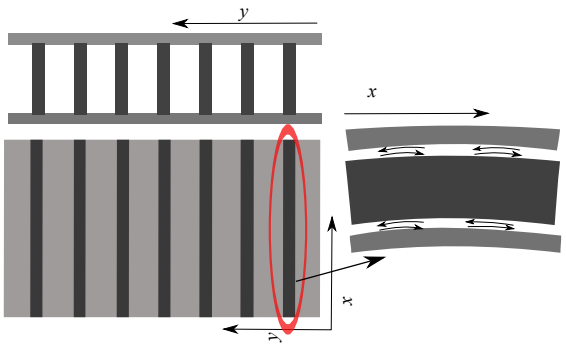

Figure 2. Depiction of the DLP model. As the plates the beam bend, there is some slippage along the junction as shown in the drawing on the right.

The beams will be modelled using the Euler beam theory. Thus the strain and kinetic energy contributions from the beams are

$$\mathscr{V}_2 = \frac{1}{2}\sum_{j=1}^{S}\int_0^A D_2\left|w_2''(x,j)\right|^2 dx, \tag{5}$$

$$\mathscr{T}_2 = \frac{\rho_2 h_2 \omega^2}{2}\sum_{j=1}^{S}\int_0^A |w_2(x,j)|^2 dx \tag{6}$$

where D_2 is the rigidity of the beam and ρ_2 and h_2 are the mass density per unit length and the thickness of the beam, respectively. Note that the primes on w_2 indicate the second derivative with respect to x. Here D_2 is assumed to constant and calculated using the formula $D_2 = E_2 h_2^3 l/12$, where E_2, h_2 and l are the Young's modulus, vertical depth and horizontal width of the beam. All beams are assumed to be identical. Again the following partial differential equation for the displacement of an Euler beam may be more familiar.

$$D_2\frac{d^4 w_2}{dx^4}(x,j) - \omega^2\rho_2 h_2 w_2(x,j) = p_1(x) - p_3(x) \tag{7}$$

for $j = 1,2,...,S$ where p_1 and p_3 are the forces from the top and the bottom plates, respectively. It is assumed that the plates and the beams are in constant contact, and thus the conditions are $w_1(x,y_j) = w_2(x,j) = w_3(x,y_j)$.

One can include the energy contributions from the junctions between the plates and the beams due to the discrepancy in the displacement of the two components (see Figure 2). This discrepancy is called the slippage. The energy contribution from the junctions is given by

$$\mathscr{P}_{1,2} = \frac{1}{2}\sum_{j=1}^{S}\int_0^A \sigma_j(x)\left|h_1 w_1'(x,y_j)\right. \\ \left. + h_2 w_2'(x,j)\right|^2 dx \tag{8}$$

where σ is the Hooke's constants (though it is a function of x) for resistance for the slippage at the junction. Note that the amount of slippage is the sum of the lateral displacement of the two plate because the lateral displacement of a thin plate (and beam) is determined solely by the vertical displacement of the mid-plane. Hence the respective surfaces of the plate and the beam move in the opposite direction as the plate and the beam bend. The above equation can be simplified using the contact condition. Then the energy is

$$\mathscr{P}_{1,2} = \frac{\tilde{h}^2}{2}\sum_{j=1}^{S}\int_0^A \sigma_j(x)\left|w_1'(x,y_j)\right|^2 dx \tag{9}$$

where $\tilde{h} = h_1 + h_2$. The contribution from the beams and the bottom plate have the same formula except that the notation is $\mathscr{P}_{2,3}$ with the displacement functions w_2 and w_3. Finally the modified variational form from Equation (1) is then given by

$$\delta^{(1)}\left[\mathscr{T} + \mathscr{P}_{1,2} + \mathscr{P}_{2,3} - \mathscr{V} - \mathscr{U}\right] = 0 \tag{10}$$

Now the terms $\mathscr{T}$ and $\mathscr{V}$ are the sum of all kinetic and strain energies of the plates and the beams.

Fourier series solution

The method of solution used for equation (10) in this paper is the Fourier expansion method because of the rectangular shape of the structure. The displacement $w(x,y)$ can be expressed as products of Fourier modes in the x and y directions. Furthermore the boundary of the plate is assumed to be simply supported. Thus the basis functions are sine-functions, which further simplifies the derivation of the solution. Different basis functions must be chosen when the boundary conditions are different. There are a few example sets of basis functions shown in (Shames and Dym, 1991) for free or clamped boundaries. Whatever the basis functions may be, a linear system of equations for the coefficients of the expansion will need to be derived and solved. Hence the method of solution shown here will be applicable. This section will show the derivation for the DLP because the single plate case is a simpler version of the DLP.

The displacement of the top plate can be expressed by

$$w_1(x,y) = \sum_{m,n,=1}^{N} C_{mn}^{(1)}\phi_m(x)\psi_n(y) \tag{11}$$

and the beams by

$$w_2(x,j) = \sum_{m=1}^{N} C_{mj}^{(2)}\phi_m(x) \quad j = 1,2,...,S, \tag{12}$$

where the basis functions are

$$\phi_m(x) = \sqrt{2/A}\sin k_m x, \quad \psi_n(y) = \sqrt{2/B}\sin\kappa_n y \tag{13}$$

The series for the bottom plate w_3 is same as Equation (11) except the sub- and super-scripts are changed from 1 to 3. The wavenumbers are given by $k_m = \pi m/A$ and $\kappa_n = \pi n/B$. Note that the basis functions are orthonormal. The positions of the joists are given by $y = y_j$, $j = 1,2,...,S$. The equations for the coefficients $\{C_{mn}^{(1)}, C_{mj}^{(2)}, C_{mn}^{(3)}\}$ are derived by substituting the series expansions into Eqs. (3), (6), (8) and then into Equation (10). Note that the number of terms in the series has already been truncated to N to construct the finite system for the numerical computation.

The terms in Equation (10) can be expressed using the column vectors of the coefficients, which are

$$\mathbf{c}_1 = \left(C_{11}^{(1)}, C_{21}^{(1)}, \cdots, C_{NN}^{(1)}\right)^{\mathrm{T}}$$
$$\mathbf{c}_2 = \left(C_{11}^{(2)}, C_{21}^{(2)}, \cdots, C_{NS}^{(2)}\right)^{\mathrm{T}}$$
$$\mathbf{c}_3 = \left(C_{11}^{(3)}, C_{21}^{(3)}, \cdots, C_{NN}^{(3)}\right)^{\mathrm{T}}$$

or simply denoted by the column vector $\mathbf{c} = (\mathbf{c}_1, \mathbf{c}_2, \mathbf{c}_3)$. The superscript 'T' denotes the vector transpose. The variational formulation then becomes

$$\delta^{(1)}\left\{\frac{1}{2}\mathbf{c}^{\mathrm{t}}\mathbf{L}\mathbf{c} - \mathbf{p}^{\mathrm{t}}\mathbf{c}\right\} = 0 \tag{14}$$

where $\mathbf{L}$ is the matrix from the integrals and $\mathbf{p}$ is the vector of the external forcing and the super-script t indicates the vector transpose. The elements of $\mathbf{p}$ are given by the integral in Equation (4),

$$\int_0^A \int_0^B p(x,y)\phi_m(x)\psi_n(y)\,dxdy \tag{15}$$

for $m,n = 1,2,...,N$ with zero padding for the parts corresponding to $\mathbf{c}_2$ and $\mathbf{c}_3$ and thus the bottom $N^2+N\times S$ elements are zero. In the numerical computations, the forcing will be set to be a point forcing, that is, $p(x,y) = \delta(x-x_0, y-y_0)$ for some fixed point (x_0, y_0), and thus the integrals are unnecessary. The coefficients are then found by solving the normal equation of Equation (14),

$$\mathbf{Lc} = \mathbf{p} \tag{16}$$

Contact conditions between the plates and the beams

The irregularity in the contact between the plates and the beams can be included by changing the function $\sigma(x,j)$ in Equation (9). Substituting the Fourier series expansion for the displacements w_1 and w_2 into Equation (9) gives

$$\mathscr{P}_{1,2} = \frac{1}{2}\sum_{j=1}^{S}\int_0^A \sigma(x,j)\left| h_1 \sum_{m,n=1}^{N} k_m C_{mn}^{(1)} \varphi_m(x)\psi_n(y_j) + h_2 \sum_{m=1}^{N} k_m C_{mj}^{(2)} \varphi_m(x)\right|^2 dx \tag{17}$$

where $\varphi_m(x) = \sqrt{2/A}\cos k_m x$. The above integral can be separated into the terms that involving the pairs $\left(C_{mn}^{(1)}, C_{mn}^{(1)*}\right)$, $\left(C_{mj}^{(2)}, C_{mn}^{(2)*}\right)$, and $\left(C_{mn}^{(1)}, C_{mj}^{(2)*}\right)$, where $*$ indicates the complex conjugate. The contribution from the junctions are

$$\begin{aligned}\mathscr{P}_{1,2} =& \frac{1}{2}\sum_{j=1}^{S}\sum_{\substack{m,n,\\ m',n'=1}}^{N} h_1^2 C_{mn}^{(1)} C_{m'n'}^{(1)*} \psi_n(y_j)\psi_{n'}(y_j) J_{mm'} \\ &+ \frac{1}{2}\sum_{j=1}^{S}\sum_{m,m'=1}^{N} h_2^2 C_{mj}^{(2)} C_{m'j}^{(2)*} J_{mm'} \\ &+ \mathrm{Re}\sum_{j=1}^{S}\sum_{\substack{m,m',\\ n=1}}^{N} h_1 h_2 C_{mn}^{(1)} C_{m'j}^{(2)*} \psi_n(y_j) J_{mm'}\end{aligned}$$

where

$$J_{mm'} = k_m k_{m'} \int_0^A \sigma(x,j)\varphi_m(x)\varphi_{m'}(x)\,dx \tag{18}$$

The above integrals and summations can be rewritten using the vectors $\mathbf{c}_1$ and $\mathbf{c}_2$ and a matrix denoted by $\mathbf{L}_\sigma$,

$$\mathscr{P}_{1,2} = \frac{1}{2}\begin{pmatrix}\mathbf{c}_1\\ \mathbf{c}_2\end{pmatrix}^{\mathrm{t}} \left[\begin{array}{c|c} \mathbf{L}_1^\sigma & \mathbf{L}_{1,2}^\sigma \\ \hline \mathbf{L}_{2,1}^\sigma & \mathbf{L}_2^\sigma \end{array}\right] \begin{pmatrix}\mathbf{c}_1\\ \mathbf{c}_2\end{pmatrix} \tag{19}$$

Note that $\mathbf{L}_{1,2}^\sigma = \left(\mathbf{L}_{2,1}^\sigma\right)^*$. The matrices $\mathbf{L}^\sigma$'s will be a part of the matrix $\mathbf{L}$ in Equation (14). Finally the linear system can be assembled from the energy contributions from all individual components (Equation (19)).

$$\left[\begin{array}{c|c|c} \mathbf{L}_1+\mathbf{L}_2^\sigma & \mathbf{L}_{1,2}^\sigma & 0 \\ \hline \mathbf{L}_{2,1}^\sigma & \mathbf{L}_2+\mathbf{L}_2^\sigma & \mathbf{L}_{2,3}^\sigma \\ \hline 0 & \mathbf{L}_{3,2}^\sigma & \mathbf{L}_3+\mathbf{L}_3^\sigma \end{array}\right] \begin{pmatrix}\mathbf{c_1}\\ \mathbf{c_2}\\ \mathbf{c_3}\end{pmatrix} = \mathbf{p}$$

The zero parts come from the fact that the effects of the cavity air is neglected, and thus there is no direct interaction between the top and the bottom plates.

NUMERICAL COMPUTATION OF SOLUTIONS

Simulating random functions

The previous sections have shown how the inhomogeneous rigidity and junctions can be included in the model. This section shows how to generate random numbers and functions for these parameters. A simple discrete case is considered when the plate is divided into the grid as shown in Figure 1 with a constant rigidity $\{D_{pq}\}_{p=1,...,P,q=1,...,Q}$, assigned for each grid. These sets of random numbers are assumed to be independent and have an identical PDF. Hence the values for D_{pq} can simply be generated using a random number generator on a computer.

In addition to the discrete rigidity, continuous smooth functions for the rigidity and the slippage are also tested. In other words, the rigidity $D(x,y)$ in Equation (3) can be rewritten to have a constant part and a zeros-mean random part. The rigidity is

$$D(x,y) = \overline{D} + d(x,y) \tag{20}$$

where $\overline{D}$ is the average rigidity and $d(x,y)$ is the random deviation. The slippage resistance function can also be expressed with the average and random deviation parts,

$$\sigma_j(x) = \overline{\sigma} + S(x) \tag{21}$$

Note that the index j is omitted because the resistance for all beams will be randomized in the same way. These functions must be simulated with some PDF and PSD. A 1-dimensional random function (process) $S(x)$ is considered first. A parameter function with any PDF can be simulated using the method given in (Kay, 2010). However here only the Gaussian density function will used. When the PSD of the parameter function is given by $P_S(f)$, the realizations of $S(x)$ with PDF $p_S(x)$ are derived by the following procedures. The following derivation is virtually identical to that of (Kay, 2010), and repeated here to keep this paper self-contained.

The methods of generating continuous smooth random functions have been studied by the signal processing community for many years (see (Grigoriu, 1998; Shinozuka, 1971)). Here the random functions are simulated using the method given in (Kay, 2010), in which a stationary random process is simulated using a prescribed PDF and PSD. As an example, the Gaussian distribution is used for the prescribed PDF here. There are two reasons for the choice of Gaussian distribution. First, the computation of normally distributed random functions is simple. Second, the author has not been able to find any measurements of the PDF of stiffness of timber products and their junctions, which are the components that make up the DLP here.

Let $S(x)$ be a random function (or random process) for the spatial variable $0 \le x \le A$. It is assumed that $S(x)$ has the probability $p(S \le s)$ and the PDF $p_S(s)$ at any $x \in [0,A]$. The PDF $p_S(s)$ is assumed to be identical for any x. In other words $S(x)$ is a stationary process. It is further assumed that $S(x)$ can be expressed by

$$S(x) = \sqrt{\frac{2}{M}}\sum_{i=1}^{M} Q_i \cos(2\pi F_i x + \Phi_i) \tag{22}$$

where Q_i, F_i, and Φ_i are the random variables with some probability densities. Here M needs to be sufficiently large, and is set to 100. The above series makes the mean of $S(x)$ zero for all $x \in [0,A]$. The procedure given in (Kay, 2010) is followed to formulate the PDFs for Q_i, F_i, and Φ_i.

First, the amplitudes $\{Q_i\}$ are assumed to be independent and identically distributed (i.i.d) random variable with PDF denoted by $p_Q(q)$ for $q > 0$. The phases $\{\Phi_i\}$ are also assumed to be i.i.d and their PDF is given by the uniform distribution in $[-\pi,\pi]$. The frequencies $\{F_i\}$ are i.i.d with the marginal first order continuous PDF denoted by $p_F(f)$ for $0 \le f \le V/2$.

The PDF of F_i and the PSD of $S(x)$ denoted by $P_S(f)$ are related by the formula

$$p_F(|f|) = \frac{2}{\mathbb{E}\left[Q^2\right]} P_S(f) \tag{23}$$

Setting the variance of S to be v^2 gives $\mathbb{E}\left[Q^2\right] = v^2$. The PSD function $P_S(f)$ here is chosen to be simple bell shaped, for example, $P_S(f) = K\exp\left(-(f-\delta)^2/2\mu^2\right)$, where K, δ, and μ will be varied to simulate effects of changing parameters. An example is shown in Figure 4(left).

The characteristic function of the random function $S(x)$ is given by

$$\begin{aligned}\psi_S(\gamma) &= \mathbb{E}\left[e^{i\gamma S}\right] \\ &= \left[\int_0^\infty p_Q(q) J_0\left(\frac{\gamma q}{\sqrt{M/2}}\right) dq\right]^M \end{aligned} \tag{24}$$

where J_0 is the Bessel function of the first kind of order zero. The PDF for Q is related to the characteristic function of $S(x)$ by

$$p_Q(q) = q\int_0^\infty \left(\psi_S(v\sqrt{M/2})\right)^{1/M} J_0(qv)v\,dv$$

which is the inverse Hankel transform. For the Gaussian parameter, the characteristic function is given by $\psi_S(\gamma) = \exp\left(-v^2\gamma^2/2\right)$. Hence the inverse Hankel transform gives the following PDF of the amplitude

$$p_Q(q) = q\int_0^\infty \left(\exp\left(-\frac{Mv^2}{4}v^2\right)\right)^{1/M} J_0(qv)v\,dv$$

The above integral has the closed form, which is

$$p_Q(q) = \frac{2q}{v^2}\exp\left(-\frac{q^2}{v^2}\right) \tag{25}$$

This is a Rayleigh PDF, which can be simulated from the two Gaussian random variables. For example, when the variance is $v^2 = 2$, then the amplitudes are simulated by $U_1 \sim \mathcal{N}(0,1)$ and $U_2 \sim \mathcal{N}(0,1)$, then $Q \sim \sqrt{U_1^2 + U_2^2}$. The slippage function $S(x)$ will be generated using the distribution shown in Figure 3 and the PSD in Figure 4(left). The standard deviation of the distribution will be set to be 10% of the average slippage resistance constant 3×10^7 Nm^{-1}. This average value comes from the experimental measurements in (Chung and Emms, 2008) for the junction between a plywood panel and a timber joist.

The random rigidity function $d(x,y)$ can be similarly simulated using the expansion

$$d(x,y) = \sqrt{\frac{2}{M}}\sum_{i=1}^{M} Q_i \cos\left(2\pi F_i x + 2\pi G_i y + \Phi_i\right)$$

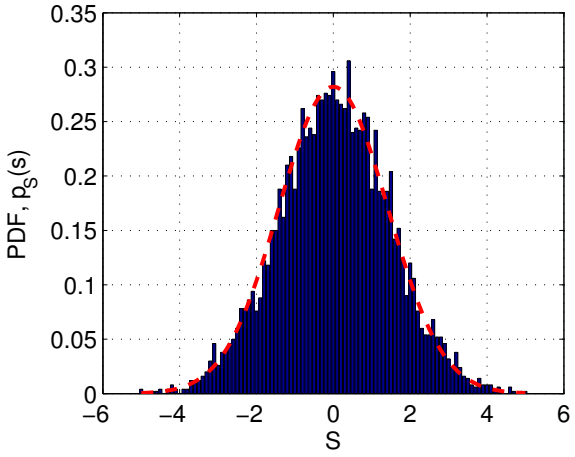

Figure 3. The PDF of $S(x)$. The target PDF is shown in dotted line.

where the coefficients $\{Q_{ij}\}$ are random variables with the Rayleigh distribution, and Φ_i and Ψ_j are uniformly distributed random values in $[-\pi,\pi]$. The frequencies F_i and G_j are also generated from Equation (23) and Equation (24). In order to prove that the above expression correctly simulates the random realization in 2-dimensional space with the correct PSD and PDF, one needs to extend the derivation given in (Kay, 2010), which is beyond the scope of this paper. Instead only the simulated realizations are numerically confirmed here. Again the PSD of d_1 (and d_3) is chosen to be a simple bell shaped function. An example is shown in Figure 4(right). In the numerical simulations, the standard deviation of the rigidity of the plates $d_1(x,y)$ and $d_3(x,y)$ will be set to be 10% of the average stiffness of the plates in the following section.

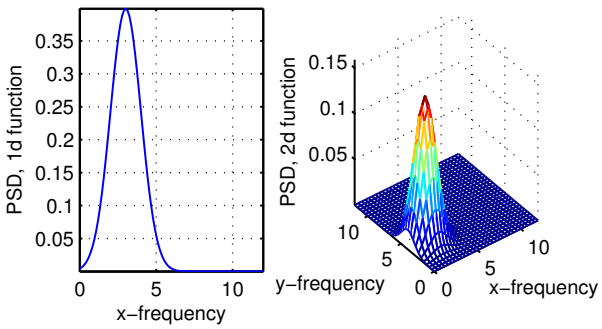

Figure 4. Examples of PSDs for the 1 and 2 dimensional random functions

Parameters for the computations

The number of terms for the Fourier expansion was set to be $N = 20$. All computation results are produced using MatLab on a standard desktop PC. The parameters for the beams and the plates are chosen from the well used values for plywood and timber beams, $E_1 = E_3 = 10^{10}$ Pa, $E_2 = 1.4\times10^{10}$ Pa, $m_1 = m_2 = m_3 = 500$ kgm^{-3}, $A = 1.5$ m, $B = 2.5$ m, $h_1 = h_3 = 0.015$ m, $h_2 = 0.1$ m, $v = 0.3$, $y_j = jB/6$, $j = 1,2,...,5$, and the width of the beams is 0.05m. The damping is not considered. The average slippage constant is 3×10^7 Nm^{-1}, which was determined from the experiments in (Chung and Emms, 2008). The location of the forcing is $(1.07, 1.67)$ with

$f_0 = 1000$ N. The range of the frequency is from 1 Hz to 1000 Hz with 0.5 Hz intervals.

Eigenvalue analysis

For the single-plate cases, analysing the natural frequencies of the random plate lets one compare the effects of the random rigidity. The three cases of random rigidities are considered here. First, $D_{pq} \sim U(-1,1)$, i.e., D_{pq} has the uniform PDF in $[-1,1]$. Second, $D_{pq} \sim \mathcal{N}(0,1)$, i.e., D_{pq} has the Gaussian PDF with zeros mean and the standard deviation of 1. For these two cases $\{D_{pq}\}$ are assumed to be uncorrelated. Third, $d(x,y)$ at any (x,y) has the independent identical Gaussian probability density function, and the function d has the bell-shaped power spectral density function over $(x,y) \in [0,A] \times [0,B]$.

Figure 5 shows the mean fundamental frequencies α_n, $n = 1,2,...,100$ and their variance computed from the eigenvalues of the stiffness matrix. The mean of α_n is computed for the discrete and smooth rigidities. The PDFs of the discrete rigidity made little difference, whereas the smooth rigidity diverges as the frequency increases. The amount of variance of the fundamental frequencies increases linearly for both uniformly and normally distributed rigidity as n increases. The smooth rigidity gives larger variance compared to the discrete cases when the standard deviation is the same 10% of the average rigidity.

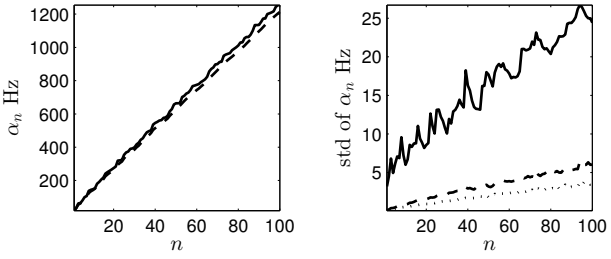

Figure 5. On the left, the mean of the fundamental frequencies for the discrete (solid) and the smooth (dashed) random rigidities. On the right, the standard deviation of the fundamental frequencies for uniformly distributed (dotted), normally distributed (dashed) and the smooth (solid) random rigidities. The standard deviation of all three cases is 10% of the average rigidity $\overline{D}$.

Figure 6 shows the PDFs of α_{50} for the uniform, normal and smooth rigidities. The other $\{\alpha_n\}$ had the similar distribution. The fundamental frequency due to the discrete rigidities is normally distributed. Whereas α_{50} due to the smooth random rigidity has a skewed distribution. A set of examples are shown in Figure 6. The skewness (always negative) increases as n increases.

Figures 7 and 8 show the fundamental frequencies when the slippage σ_j and the stiffness d_1 and d_3 are randomized. Because of the multiple components, there are more fundamental frequencies than the single-plate case. The mean fundamental frequencies shows no difference between the two random functions. However, the slippage affects the fundamental frequencies more than the rigidity. In both cases, the deviation does not grow linearly as the single-plate case shown in Figure 5. The difference in the effects of the slippage and the rigidity is also shown in the transmission-loss studies in the next section.

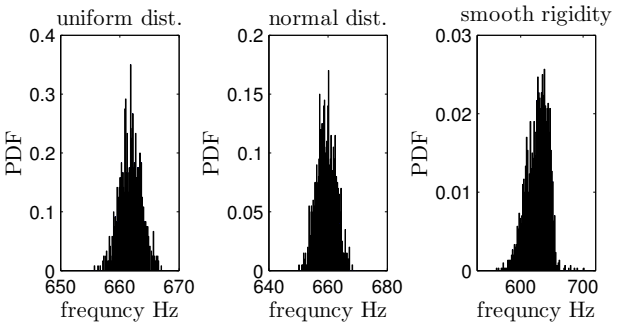

Figure 6. The PDF of 50th fundamental frequency for the uniform distribution (right), normal distribution (center) and smooth rigidity (right).

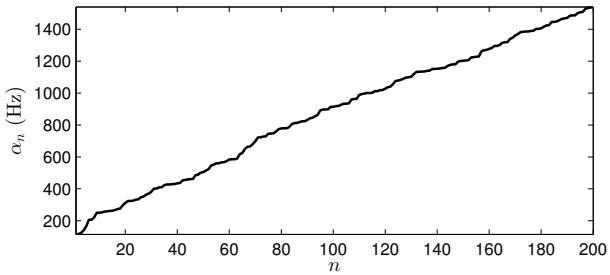

Figure 7. The mean of the fundamental freqeuncies of the DLP.

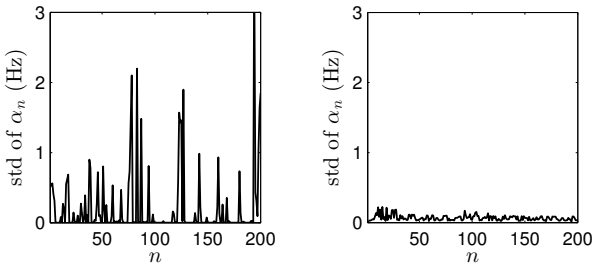

Figure 8. The standard deviation of the fundamental freqeuncies when slippage is randomized (left) and the rigidity of the plates is randomized (right).

Transmission-loss analysis

This section shows the behaviour of the DLP using the transmission-loss (TL) between the top plate and the bottom one. The root-mean-square velocity (RMSV) of the plates are computed from the displacement w_1 and w_3, and then the TL of the DLP for various cases of random parameters are compared. The TL in this case is a simple log-ratio between the RMSV of the top and the bottom plates.

The linearity of the system leads to the velocity of the plate by $v_1(x,y) = \mathrm{i}\omega w_1(x,y)$ (or $\mathrm{i}2\pi\alpha w_1(x,y)$) and same for v_3. Hence the RMSV can be computed by

$$\sqrt{\langle |v|^2 \rangle} = \frac{1}{\sqrt{AB}} \left[\int_0^B \int_0^A \omega^2 \, |w(x,y)|^2 \, dxdy \right]^{1/2}$$

The above integral can be obtained using the simple Riemann sum once the displacement $w_1(x,y)$ and $w_3(x,y)$ have been

computed. Here the TL is defined as the energy-loss ratio that occurs as the vibration travels from one plate to the other plate in an surface averaged sense. The usual calculation of the transmission loss includes the ratio of the mass densities of the plates and requires the plates to be homogeneous, which is not the case here. The term 'TL' is used for its convenience. The TL is a function of frequency α, which is computed by

$$TL(\alpha) = \log_{10}\left[\sqrt{\langle|v_1|^2\rangle}\Big/\sqrt{\langle|v_3|^2\rangle}\right] \tag{26}$$

Note that the mass density of the two plates are equal here.

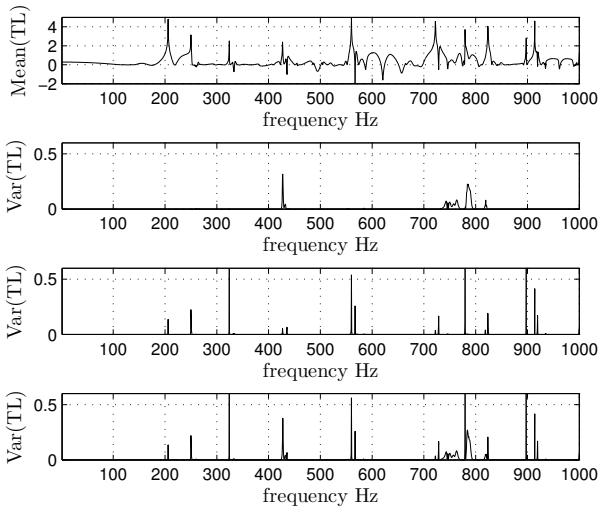

Figure 9. The mean of the TL (top). The variance of the TL when the slippage alone is randomized (top second), rigidity alone is randomized (top third) and both the slippage and the rigidities are randomized (bottom).

Here two cases are considered when the slippage alone is randomized and both the slippage and the rigidity (both the top and the bottom plates) are randomized. The standard deviation of the slippage $S(x)$ in Equation (21) is set to be 30% of the average slippage constant $\overline{\sigma}$. The random rigidities $d_1(x,y)$ and $d_3(x,y)$ are the same as before, which are set at 10% of the average rigidity. The TL and the variance of the TL are shown in Figure 9. The mean of the TL changed little regardless of the randomization, and thus the smoothness of the rigidity made no difference to the mean TL. The variance of the surface velocity itself was much smaller than the single-plate cases shown in the previous section. The variance of the TL increases as the random rigidity is introduced the DLP, though the variance has appreciable values mostly at the maxima of TL. The random rigidity affects the TL over a wider frequency range than the random slippage does.

SUMMARY

The simulations of the vibration of elastic plates with random parameters have been carried out using the variational principle and the Fourier series expansion method. A single plate and a DLP have been considered. For the single plate, discrete and smooth rigidities are used to simulate their effects on the fundamental frequencies. The smooth rigidity gives larger variations in the fundamental frequencies than the discrete ones. Furthermore the distribution of the fundamental frequencies is skewed when the smooth rigidity is used. On the other hand, the discrete rigidities give normally distributed fundamental frequencies. The model for the DLP includes the inhomogeneous junctions between the beams and the plates. The random slippage and the random rigidity are simulated from a pre-assigned PDF at each location and a PSD over either the beam or the plate. The TL is then used to study the effects of the randomness. The computational cost of computing the whole displacement and the average velocity is kept small using the Fourier series solutions and the variational formulation. The simulations of the eigenvalues and the TL show that the random $d_1(x,y)$ (and d_3) affects the DLP much less than it does the single plate. The mean of the TL remains the same regardless of the varying randomness in the slippage and the rigidity. The slippage affects narrower range of frequencies than the rigidity does.

REFERENCES

Brunskog, J 2005, 'The influence of finite cavities on the sound insulation of double-plate structures', *Journal of the Acoustical Society of America*, vol. 117, no. 6, pp. 3727–3739.

Brunskog, J & Chung, H 2011, 'Non-diffuseness of vibration fields in ribbed plates', *Journal of the Acoustical Society of America*, vol. 129, no. 3, pp. 1336–1343.

Chung, H 2012, 'Vibration field of a double-leaf plate with random parameter functions', *Acoustics Australia*, vol. 40, no. 3, pp. 203–210.

Chung, H & Emms, G 2008, 'Fourier series solutions to the vibration of rectangular lightweight floor/ceiling structures', *Acta Acustica United With Acustica* vol. 94, no. 3, pp. 401–409.

Craik, R 2000, 'Sound transmission through double leaf lightweight partitions. Part I: airborne sound', *Applied Acoustics*, vol. 61, pp. 223–245.

Craik, R 2000, 'Sound transmission through double leaf lightweight partitions. Part II: structure-borne sound', *Applied Acoustics*, vol. 61, pp. 247–269.

Fahy, F 1994, 'Statistical energy analysis: A critical overview', *Philosophical Transactions of the Royal Society of London. Series A: Physical and Engineering Sciences*, vol. 346, no. 1681, pp. 431–447.

Grigoriu, M 1998, 'Simulation of stationary non-gaussian translation processes', *Journal of engineering mechanics*, vo. 124, no. 2, pp. 121–126.

Hodges, C & Woodhouse, J 1986, 'Theories of noise and vibration transmission in complex structures', *Reports On Progress In Physics* vol. 49, no. 2, pp. 107–170.

Kay, S 2010, 'Representation and generation of non-Gaussian wide-sense stationary random process with arbitrary PSDs and a class of PDFs', *IEEE Trans. Signal Processing,* vol. 58, no. 7, pp. 3448–3458.

Lyon, R 1975, *Statistical energy analysis of dynamical systems: theory and applications*, New York: MIT Press.

Mace, B 1980, 'Periodically stiffened fluid-loaded plates, I: Response to convected harmonic pressure and free wave propagation', *Journal of Sound and Vibration*, vol. 73, no. 4, pp. 473–486.

Mace, B 1980, 'Periodically stiffened fluid loaded plates, II: Response to line and point forces', *Journal of Sound and Vibration*, vol. 73, no. 4, pp. 487–504.

Mace, B 1980, 'Sound radiation from a plate reinforced by two sets of parallel stiffeners', *Journal of Sound and Vibration*, vol. 71, no. 3, pp. 435–441.

Shames, I & Dym, C 1991, *Energy and finite element methods*

in structural mechanics (SI units ed ed.). New York: Taylor & Francis.

Shinozuka, M 1971, 'Simulation of multivariate and multidimensional random process', *Journal of the Acoustical Society of America*, vol. 49, no. 1, pp. 357–368.

Wang, J & Lu, T & Woodhouse, J & Langley, R & Evans, J 2005, 'Sound transmission through lightweight double-leaf partitions: theoretical modelling', *Journal of sound and vibration*, vol. 286, no. 4, pp. 817–847.